UDC 551.509.313

Forecasting With a Global, Three-Layer, Primitive-Equation Model

LLOYD W. VANDERMAN—*National Meteorological Center, National Weather Service, NOAA, Suitland, Md.*

ABSTRACT—A global, three-layer, primitive-equation forecast model in spherical and σ coordinates on a 3.75° latitude-longitude grid has been developed. It has a boundary layer and two layers in the troposphere, with the top of the troposphere and top of the model atmosphere coinciding at 100 mb. This is a modified and simplified version of the National Meteorological Center six-layer, operational forecast model. Mountains, radiation, sea-surface heating, convective adjustment, and ground-surface friction are incorporated. Initial data are generated from global analyses of winds and heights on seven pressure surfaces using Hough functions. The forecast model is described in detail, and examples of the forecasts and analyses extracted from the global grid and converted to Northern and Southern Hemisphere and tropical belt map bases are displayed and discussed.

1. INTRODUCTION

Development of global forecasting capabilities at the National Meteorological Center (NMC) in support of anticipated World Weather Center requirements began in the middle 1960s. Because of the inadequacies of known and existing global forecast calculation schemes, development of a new one (Vanderman 1967) seemed necessary and was begun. Concurrent with this developmental work, others at NMC tested some of the other global calculation schemes (Dey 1969) and studied some of the problems involved (Shuman 1970). By the middle of 1969, development of an apparently successful and usable global forecast calculation scheme (Vanderman 1970, Staff, NMC 1970) was for the most part completed. Subsequently, some minor changes and improvements have been made. This scheme is described in some detail in section 3. Development and programming of a simplified (e.g., no stratospheric calculations, fewer layers, etc.), three-layer version of the NMC six-layer, operational, primitive-equation forecast model (Shuman and Hovermale 1968) was begun in early 1970. Successful calculations with test data began in September 1970. Since then, convective adjustment and simple versions of radiation effects and friction have been incorporated. Moisture and its effects are under study for inclusion later.

Independently of the previously described development, but also at NMC, Flattery (1971) developed a program for calculating integrated height, wind, and temperature analyses for 13 pressure levels from 1000 to 30 mb for a hemisphere, using Hough functions. Recently, he expanded his programs to the entire globe, and on Nov. 21, 1971, he produced the first three-dimensionally integrated and computer-calculated global analysis. Data from normal meteorological sources, aircraft winds, and satellite infrared spectrometer (SIRS) reports in the Southern Hemisphere were used. This analysis for 0000 GMT on June 4, 1970, was used as initial data for a global forecast using the three-layer model.

2. MODEL CONSTRUCTION

The model is constructed as shown in figure 1 with a planetary boundary layer (a constant 100 mb in depth), two equal pressure layers in the troposphere, and the top of the troposphere and top of the model atmosphere coinciding at the constant pressure of 100 mb. The differential equations in the dimensions of spherical and σ coordinates and time are:

$$\frac{\partial u}{\partial t}+\dot{\sigma}\frac{\partial u}{\partial \sigma}+u\frac{\partial u}{\partial x}+v\frac{\partial u}{\partial y}-fv-\frac{uv}{r}\tan\phi+g\frac{\partial z}{\partial x}+c_p\theta\frac{\partial \pi}{\partial x}+F_x=0, \quad (1)$$

$$\frac{\partial v}{\partial t}+\dot{\sigma}\frac{\partial v}{\partial \sigma}+u\frac{\partial v}{\partial x}+v\frac{\partial v}{\partial y}+fu+\frac{u^2}{r}\tan\phi+g\frac{\partial z}{\partial x}+c_p\theta\frac{\partial \pi}{\partial y}+F_y=0, \quad (2)$$

$$\frac{\partial (gz)}{\partial \sigma}+c_p\theta\frac{\partial \pi}{\partial \sigma}=0, \quad (3)$$

$$\frac{\partial \theta}{\partial t}+\dot{\sigma}\frac{\partial \theta}{\partial \sigma}+u\frac{\partial \theta}{\partial x}+v\frac{\partial \theta}{\partial y}+H=0, \quad (4)$$

$$\frac{\partial p_\sigma}{\partial t}+\frac{\partial}{\partial \sigma}(\dot{\sigma}p_\sigma)+\frac{\partial}{\partial x}(up_\sigma)+\frac{\partial}{\partial y}(vp_\sigma)-\frac{vp_\sigma}{r}\tan\phi=0, \quad (5)$$

and

$$\pi=\left(\frac{p}{P}\right)^\kappa. \quad (6)$$

The dependent variables are u, v, $\dot{\sigma}$, θ, z, π, and p. The symbol p_σ is the difference in pressure with respect to

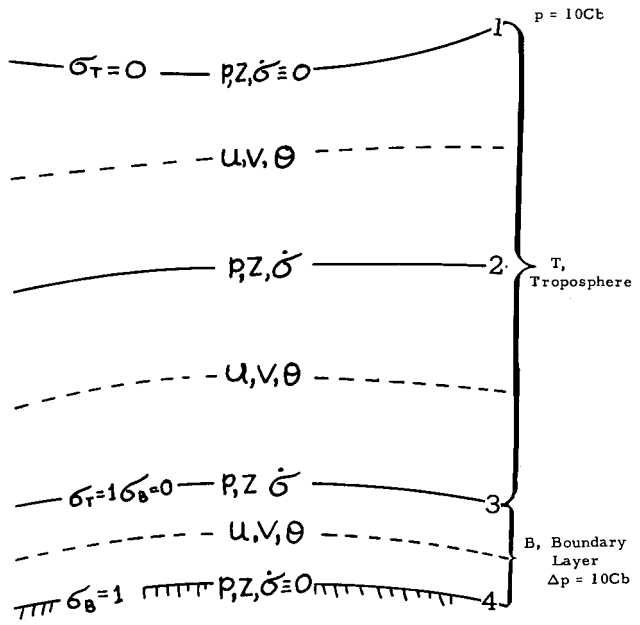

FIGURE 1.—Schematic diagram of vertical structure of the three-layer model.

σ, the vertical coordinate, for a σ domain. For the boundary layer, p_σ is a constant equal to 10 cb. For the troposphere, p_σ is the pressure difference, p_3-p_1, that is forecast. In spherical, horizontal coordinates, we have

$$\frac{\partial}{\partial x}=\frac{1}{r\cos\phi}\frac{\partial}{\partial\lambda}$$

and (7)

$$\frac{\partial}{\partial y}=\frac{1}{r}\frac{\partial}{\partial\phi}$$

where r is the earth's radius, ϕ is latitude in radians, λ is longitude in radians, t is time, u and v are the west and south wind velocity components, respectively, θ is potential temperature, z is geopotential height, p is pressure, $P=1000$ mb, $\kappa=R/c_p\approx0.287$, and f is the Coriolis parameter. F_x and F_y represent accelerations from friction, and H represents diabatic effects.

The vertical coordinate, σ, is defined for two regimes, the boundary layer, B, and the troposphere, T, as

$$\sigma_B=\frac{p-p_3}{p_4-p_3} \tag{8}$$

and

$$\sigma_T=\frac{p-p_1}{p_3-p_1}, \tag{9}$$

respectively. The pressure subscripts refer to the levels as numbered in figure 1. The notation $\dot\sigma$ represents the time derivative of σ. Since p_σ for the boundary layer is a constant and $\dot\sigma$ at the ground (level 4) is assumed to be zero, we get from eq (5), after writing the vertical difference term in finite-difference form, $\dot\sigma$ at level 3 (fig. 1 at the top of the boundary layer); that is,

$$(\dot\sigma_B)_3=\frac{\partial u_B}{\partial x}+\frac{\partial v_B}{\partial y}-\frac{v_B}{r}\tan\phi. \tag{10}$$

Subscript B denotes values in the boundary layer. The definitions of σ in eq (8) and (9) give the relation,

$$(\dot\sigma_T)_3=\frac{p_4-p_3}{p_3-p_1}(\dot\sigma_B)_3, \tag{11}$$

between $\dot\sigma$ at level 3 at the bottom of the troposphere and $(\dot\sigma_B)_3$. Taking $\partial/\partial\sigma$ of eq (5), we obtain

$$p_\sigma\dot\sigma_{\sigma\sigma}=-\left[\frac{\partial u}{\partial\sigma}\frac{\partial p_\sigma}{\partial x}+\frac{\partial v}{\partial\sigma}\frac{\partial p_\sigma}{\partial y}+p_\sigma\left(\frac{\partial}{\partial\sigma}\frac{\partial u}{\partial x}+\frac{\partial}{\partial\sigma}\frac{\partial v}{\partial y}-\frac{\partial v}{\partial\sigma}\frac{\tan\phi}{r}\right)\right], \tag{12}$$

which is used with the vertical finite-difference equations in calculating $\dot\sigma$ at level 2 of the model.

3. HORIZONTAL GRID CALCULATION

This three-layer model forecast was calculated with data from a horizontal 3.75° ($N = 24$ grid lengths from Equator to pole) latitude-longitude grid. The Equator and both poles have data points. A field consists of 4,514 (96 by 47 + 2 poles) distinct points, but it is considered to be 4,802 (98 by 49) points to allow position definition of one vector wind at each data longitude at both poles and for convenience in calculating tendencies and east–west cycling of fields. Calculation of the forecast on this 3.75° grid was carried out much the same as described for a 5.0° grid (Vanderman 1967) for a barotropic forecast model and in some detail (Vanderman 1970) for a barotropic and a version of the Phillips (1951) two-layer models.

The grid calculation scheme including some important recent revisions will be described in some detail. With the dependent variables staggered in the vertical (fig. 1) at the same points throughout the forecast calculation (e.g., at points 1, 3, 5, 7, on fig. 2), we calculated "original" tendency values at the middle of the data block (i.e., at point 9). Original tendencies are then averaged east–west to produce tendency values at center points that are on data longitudes and between data latitudes. Two of these latter values, the one to the north and the one to the south, are averaged north–south to produce the tendency value at the data point. East–west averaging involves weighting of original tendency values, two or more to the immediate east and to the immediate west, respectively, of the center point. In addition, original tendency values of wind are resolved vectorially to the orthogonal frame (local east–west, north–south) at the center point. Triangular-type weighting expressed as some inverse function, not necessarily linear, of the distance of the original tendency point from the center point at which it is being applied, gives good forecast calculation results. An earlier version employed for east–west averaging gave equal weights to original tendencies. This produced noise in the forecast fields at higher latitudes. Triangular-type weighting has eliminated this noise and, at the same time, has extended greatly the running time for a stable forecast calculation. For example, a global barotropic forecast calculation runs to 60 days using triangular-type weighting as compared to 20 days employing equal weighting.

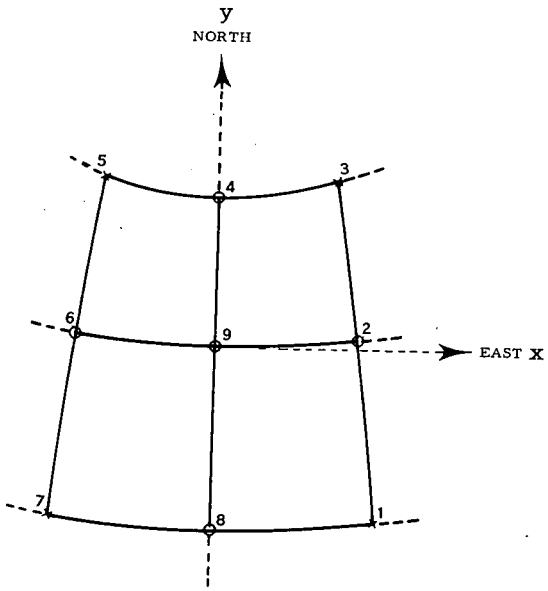

FIGURE 2.—Sample data block centered on point 9 with data points (X) at 1, 3, 5, and 7. Partial tendency values are calculated at points 2, 4, 6, and 8.

The weighting function now being employed has the form

$$W_n = 1 - \frac{n-1}{\sec \phi} \geq 0, \tag{13}$$

in which W_n is restricted to positive or zero values, ϕ is latitude, and n designates the relative position of the original tendency value with respect to the center point, counting outward both eastward and westward. In application, W_n is normalized by dividing by

$$2\sum_{1}^{N} W_n \tag{14}$$

in which N is a maximum value of n for the latitude, and the factor 2 results because an eastward set and a westward set of original tendency values are employed. N increases with latitude (sec ϕ) and at each latitude assumes the maximum value that still satisfies the imposed limit on W_n in eq (13). Even at the lowest latitude of east–west averaging, fractions of four original tendency values are employed in producing tendency values at the center points. One north–south grid length (equal to one east–west grid length at the Equator), multiplied by $\sqrt{2}$ for the diagonal grid length and then by 0.65 as a triangular-weighting consideration, approximates the length to be considered in applying the Courant-Friedrichs-Lewy stability criteria for estimating the maximum allowable time step in the forecast calculation. The 0.65 value was verified by changing the time step in a series of experimental forecast calculations.

The poles and their immediate regions receive special treatment. One vector wind is defined at a pole and is obtained initially from a vector average of the surrounding u and v components (e.g., those at 86.25° latitude on the 3.75° latitude-longitude grid). This one polar vector wind is carried at each data longitude in both u and v components resolved according to the local definition of u and v directions at the particular longitude. Initial scalar pole values are simple averages of the surrounding values. Pole tendencies are the average (scaler or u and v) tendencies (e.g., those at 88.125° latitude on the 3.75° grid in the middle of a triangular-shaped data block). The original tendency values used to produce the average polar tendency are replaced by the average polar tendency at respective longitudes, both scalars and vectors, before any east–west or north–south averaging involving these occurs. This polar treatment amounts to heavy horizontal smoothing, contributes to consistency, and allows cross-polar exchanges.

Factors considered in calculating original tendencies at the center of the highest latitude data blocks (the triangular-shaped blocks, which have one side terminating on a point at the pole) are:

1. By defining one vector wind at the pole, the tan ϕ terms and the $\partial/\partial x$ terms calculated *at* the pole cancel when paired across the pole and added appropriately as vectors or scalars. This occurs because both u and v components of velocity are equal in magnitude and opposite in sign, respectively, across the pole.

2. One vector wind at the pole dictates that a u component of velocity has the same direction and magnitude as a v component of velocity $\pi/2$ radians of longitude apart. Coriolis force, f, should multiply the pole wind one time, either u or v, but not both; f is specified zero *at* the poles as a multiplier for v in eq (17) and is retained at proper value as a multiplier for u in eq (18).

3. The term $u(\partial u/\partial x)$ in eq (1) [and eq (17)] and the term $v(\partial v/\partial y)$ in eq (2) [and eq (18)] are related. When considered as a set in calculating tendencies at the center of data blocks $\pi/2$ radians of longitude apart, they contribute vector tendencies in the same direction. Similarly related are the two terms $u(\partial v/\partial x)$ and $v(\partial u/\partial y)$.

4. Tan ϕ terms calculated (as described in factor 1) in the forms of the finite-difference equations are consistent with the other terms in the equations. This results because tan ϕ at one-half grid length from the pole is nearly twice the value at one grid length from the pole. When we produce a *pole* wind tendency (in one direction defined at the pole), the two wind tendency equations are related in the sense,

$$\overline{\left(\frac{\partial u}{\partial t}\right)_0}^{\mathrm{NP}} = \left(\frac{\partial u}{\partial t}\right)_0 - \left(\frac{\partial u}{\partial t}\right)_\pi - \left(\frac{\partial v}{\partial t}\right)_{\pi/2} + \left(\frac{\partial v}{\partial t}\right)_{3\pi/2} \tag{15}$$

and

$$\overline{\left(\frac{\partial u}{\partial t}\right)_0}^{\mathrm{SP}} = \left(\frac{\partial u}{\partial t}\right)_0 - \left(\frac{\partial u}{\partial t}\right)_\pi + \left(\frac{\partial v}{\partial t}\right)_{\pi/2} - \left(\frac{\partial v}{\partial t}\right)_{3\pi/2}, \tag{16}$$

in which the overbar indicates the sum value, NP and SP indicate North Pole and South Pole, respectively, and the subscripts indicate the relative positions of values in radians of longitude around the pole. The fact is that, in both wind tendency equations, some terms are, in a sense, missing (have zero values) and must be taken into account in performing the additions in eq (15) and (16). Although there are terms with zero values *at* the pole itself in the scalar tendency equations, adding the original tendencies

for an average pole tendency proceeds without special consideration of the terms with zero values.

4. FINITE-DIFFERENCE EQUATIONS

The block integration technique is employed to insure to the maximum that, in the calculation of original tendencies, adjacent data blocks receive equal contributions from common terms. In the following equations, used for calculating the original (middle of the data block) tendencies, the notation does not account for the east–west, north–south averaging described in section 3:

$$u_t+\overline{\dot{\sigma}_{\mathrm{NS}}\overline{u}^{y\sigma}}^{x}+\overline{\dot{\sigma}_{\mathrm{EW}}\overline{u}^{x\sigma}}^{y}+\overline{\overline{u}^{x}u_x}^{y}+\overline{\overline{v}^{y}u_y}^{x}-\overline{f_{\mathrm{NS}}\overline{v}^{y}}^{x}$$
$$-\overline{\frac{\overline{uv}^{x}}{r}(\tan\phi)_{\mathrm{NS}}}^{y}+\overline{g\overline{z}_x^{\sigma}}^{y}+\overline{c_p\overline{\theta}^{x-\sigma}\pi_x}^{y}+F_x=0, \quad (17)$$

$$v_t+\overline{\dot{\sigma}_{\mathrm{NS}}\overline{v}^{y\sigma}}^{x}+\overline{\dot{\sigma}_{\mathrm{EW}}\overline{v}^{x\sigma}}^{y}+\overline{\overline{u}^{x}v_x}^{y}+\overline{\overline{v}^{y}v_y}^{x}+\overline{f_{\mathrm{EW}}\overline{u}^{y}}^{x}$$
$$+\overline{\frac{\overline{u}^{2y}}{r}(\tan\phi)_{\mathrm{EW}}}^{x}+\overline{g\overline{z}_y^{\sigma}}^{x}+\overline{c_p\overline{\theta}^{y-\sigma}\pi_y}^{x}+F_y=0, \quad (18)$$

$$gz_\sigma+c_p\theta\pi_\sigma=0, \quad (19)$$

$$\theta_t+\overline{\dot{\sigma}_{\mathrm{NS}}\overline{\theta}_\sigma^{y\sigma}}^{x}+\overline{\dot{\sigma}_{\mathrm{EW}}\overline{\theta}_\sigma^{x\sigma}}^{y}+\overline{\overline{u}^{x}\theta_x}^{y}+\overline{\overline{v}^{y}\theta_y}^{x}+H=0, \quad (20)$$

$$p_{\sigma t}+\overline{(\dot{\sigma}_{\mathrm{NS}})_\sigma\overline{p}_\sigma^{y}}^{x}+\overline{(\dot{\sigma}_{\mathrm{EW}})_\sigma\overline{p}_\sigma^{x}}^{y}+\overline{(p_\sigma u)_x}^{y}+\overline{(p_\sigma v)_y}^{x}$$
$$-\overline{\overline{p_\sigma v}^{y}\left(\frac{\tan\phi}{r}\right)_{\mathrm{EW}}}^{x}=0, \quad (21)$$

$$[(\dot{\sigma}_B)_3]_{\mathrm{NS}}=(u_B)_x, \quad (22)$$

$$[(\dot{\sigma}_B)_3]_{\mathrm{EW}}=(v_B)_y-\overline{\frac{v_B}{r}}^{y}(\tan\phi)_{\mathrm{EW}}, \quad (23)$$

$$[(\dot{\sigma}_T)_3]_{\mathrm{NS}}=\overline{\left(\frac{p_4-p_3}{p_3-p_1}\right)}^{x}[(\dot{\sigma}_B)_3]_{\mathrm{NS}}, \quad (24)$$

$$[(\dot{\sigma}_T)_3]_{\mathrm{EW}}=\overline{\left(\frac{p_4-p_3}{p_3-p_1}\right)}^{y}[(\dot{\sigma}_B)_3]_{\mathrm{EW}}, \quad (25)$$

$$\overline{p}_\sigma^{x}(\dot{\sigma}_{\sigma\sigma})_{\mathrm{NS}}=-(\overline{u}_\sigma^{x}p_{\sigma x}+\overline{p}_\sigma^{x}u_{x\sigma}), \quad (26)$$

and

$$\overline{p}_\sigma^{y}(\dot{\sigma}_{\sigma\sigma})_{\mathrm{EW}}=-\left[\overline{v}_\sigma^{y}p_{\sigma y}+\overline{p}_\sigma^{y}v_{y\sigma}-\overline{(vp_\sigma)}_\sigma^{y}\left(\frac{\tan\phi}{r}\right)_{\mathrm{EW}}\right]. \quad (27)$$

The notation $\overline{(\ )}^{x}$ represents east–west and $\overline{(\ )}^{y}$ represents north–south averaging over one grid interval. Subscripts x and y are east–west and north–south differencing, respectively, over one grid interval. Subscripts NS and EW imply values at or calculated at points 4 and 8, and 2 and 6, respectively (fig. 2). In the model, $\dot{\sigma}$ is identically zero at the bottom of the boundary layer (at the ground) and at 100-mb pressure (the top of the model atmosphere). Considering this, that eq (26) and (27) are second-difference equations in $\dot{\sigma}$, and the vertical structure of the model, we can derive values for $\dot{\sigma}$ at the middle (level 2) of the troposphere. They are

$$[(\dot{\sigma})_2]_{\mathrm{NS}}=0.5\{[(\dot{\sigma}_T)_3]_{\mathrm{NS}}-0.25(\dot{\sigma}_{\sigma\sigma})_{\mathrm{NS}}\} \quad (28)$$

and

$$[(\dot{\sigma})_2]_{\mathrm{EW}}=0.5\{[(\dot{\sigma}_T)_3]_{\mathrm{EW}}-0.25(\dot{\sigma}_{\sigma\sigma})_{\mathrm{EW}}\}. \quad (29)$$

As examples of interpretation of these equations, we expand two terms in eq (17) as follows:

$$\overline{\overline{u}^{x}u_x}^{y}=\frac{1}{4}\left[\frac{(u_1+u_7)(u_1-u_7)}{(\Delta x)_{1,7}}+\frac{(u_3+u_5)(u_3-u_5)}{(\Delta x)_{3,5}}\right] \quad (30)$$

and

$$\overline{\overline{v}^{y}u_y}^{x}=\frac{1}{4\Delta y}[(v_3+v_1)(u_3-u_1)+(v_5+v_7)(u_5-u_7)]. \quad (31)$$

Here, Δy is one north–south grid length (3.75×111.11 km) in the 3.75° latitude-longitude grid and $\Delta x=\Delta y\cos\phi$, in which ϕ is the latitude at which Δx is being applied. The subscripts indicate numbered points in figure 2.

5. FORECAST

The forecast was calculated from 0000 GMT June 4, 1970 global analyses using Hough functions. Winds and heights at seven levels (1000, 850, 700, 500, 300, 200, and 100 mb) were used in interpolating initial winds and heights to levels 1, 2, 3, and 4 (fig. 1) of this model. The wind (u and v) at the middle of a layer was calculated as the mean of the values at the top and bottom of the layer. Potential temperature of a layer was calculated as the mean value from the height and pressure at the top and bottom of the layer. Full global and unsmoothed mountains and convective adjustment (if and when necessary) were employed. Boundary-layer heating and friction and radiation were not allowed in this particular forecast calculation. The beginning of the forecast was preceded by 6 hr of forward-backward time initialization calculation, using a Euler-backward time tendency smoother (Nitta and Hovermale 1969), during which time the mutual adjustment of all the forecast variables was allowed. Centered-in-time forecast calculations with a 900-s time step were employed. Also, time smoothing was employed at each time step in the form,

$$u_\tau^*=\alpha u_\tau+0.5(1-\alpha)(u_{\tau+1}+u_{\tau-1}^*), \quad (32)$$

in which $\alpha=0.5$ and the subscripts indicate time levels. Figures 3–6 and 11–18 are examples of the 24-hr height forecasts and initial and verifying height analyses for the Tropics, the Northern Hemisphere, and the Southern Hemisphere, respectively. Figures 7–10 are stream function charts, derived from the winds and scaled by the gravity constant divided by the Coriolis parameter value for 45° latitude. The spacing interval of lines is 60 m. The stream fields define the flow at low latitudes much better than the comparable height fields of figures 3–6. The forecast maps were constructed from bilinear interpolations to the NMC Mercator and polar stereographic grids for both hemispheres. Data vertically

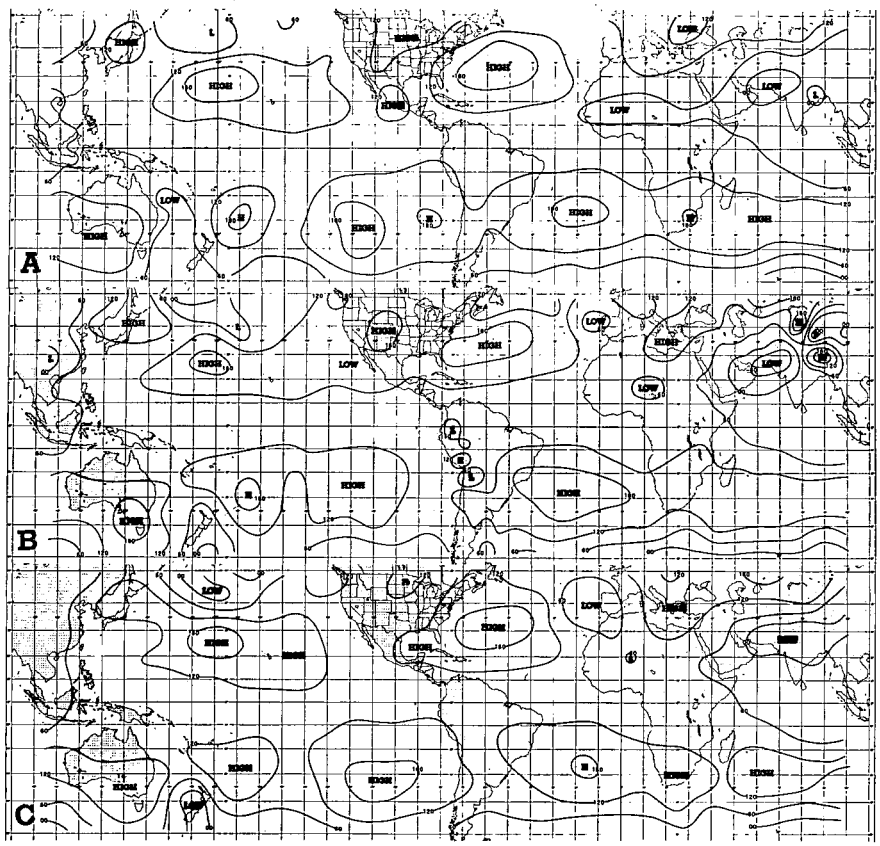

FIGURE 3.—The 1000-mb height field (m) for the tropical belt: (A) initial, 0000 GMT, June 4, 1970, (B) 24-hr forecast, and (C) verification

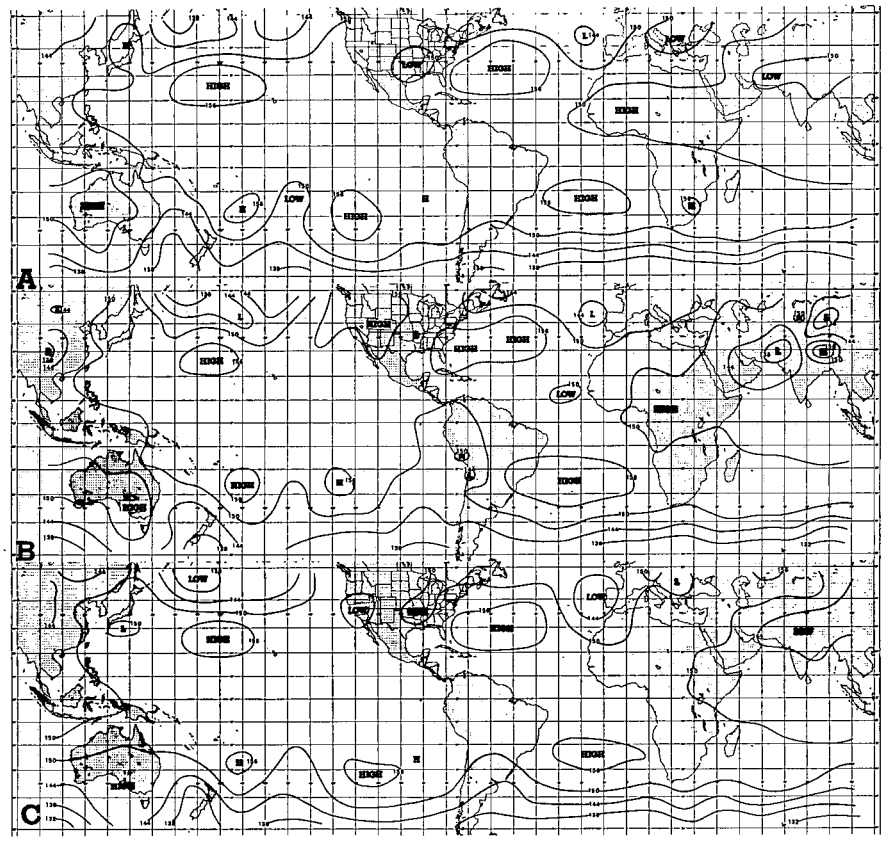

FIGURE 4.—Same as figure 3 for 850 mb.

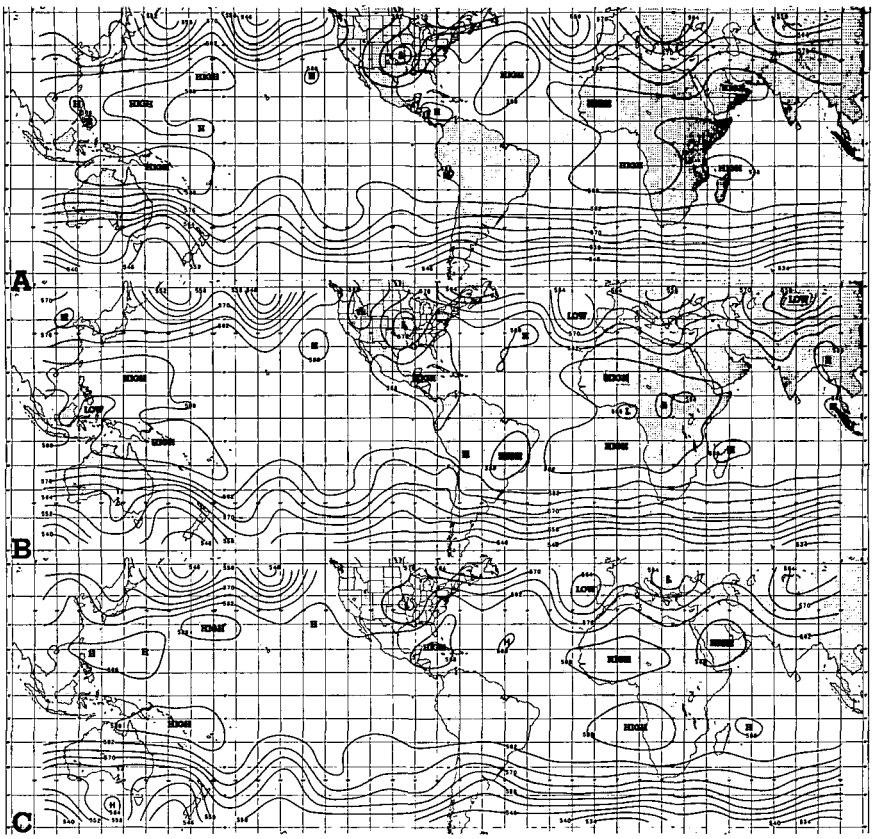

FIGURE 5.—Same as figure 3 for 500 mb.

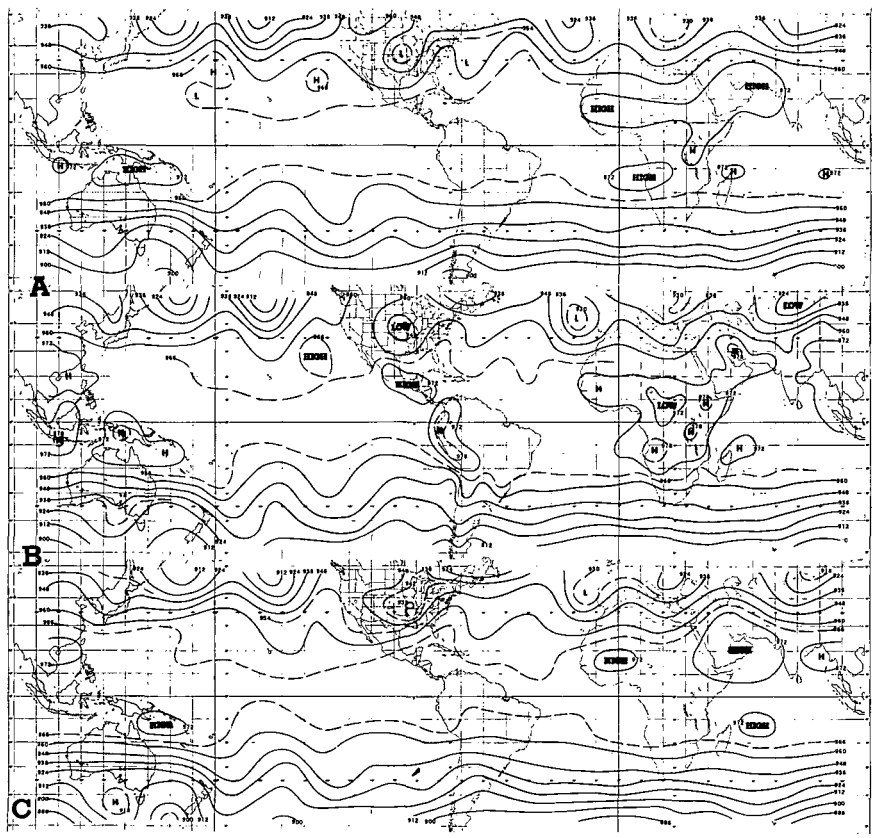

FIGURE 6.—Same as figure 3 for 300 mb.

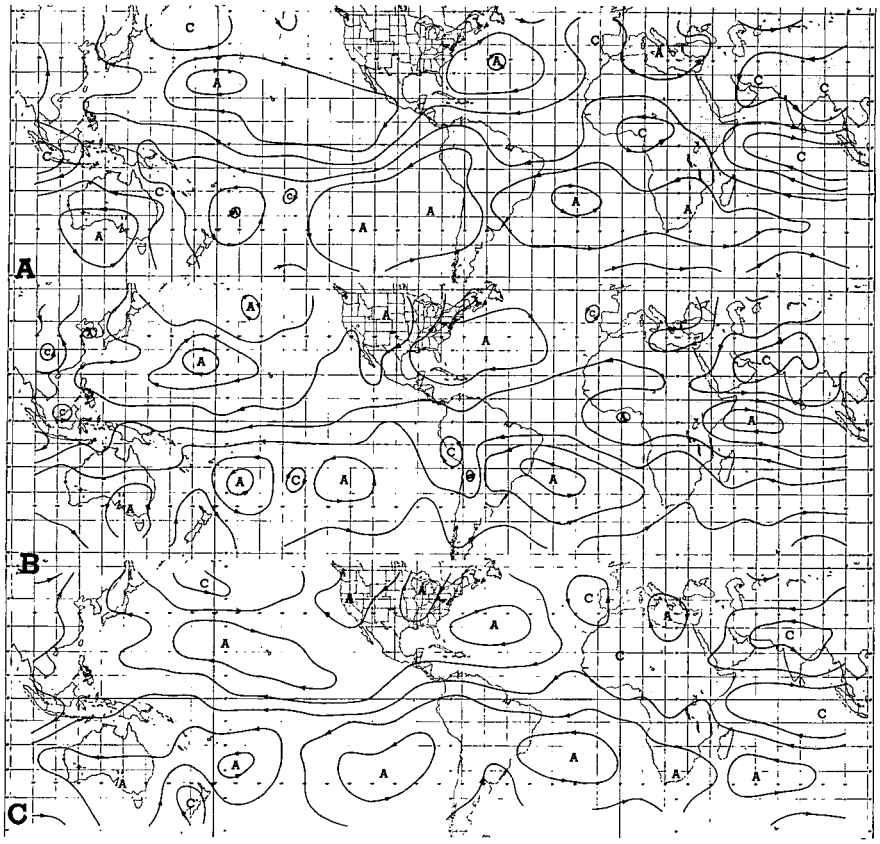

FIGURE 7.—The 1000-mb stream function for the tropical belt: (A) initial 0000 GMT, June 4, 1970, (B) 24-hr forecast, and (C) verification.

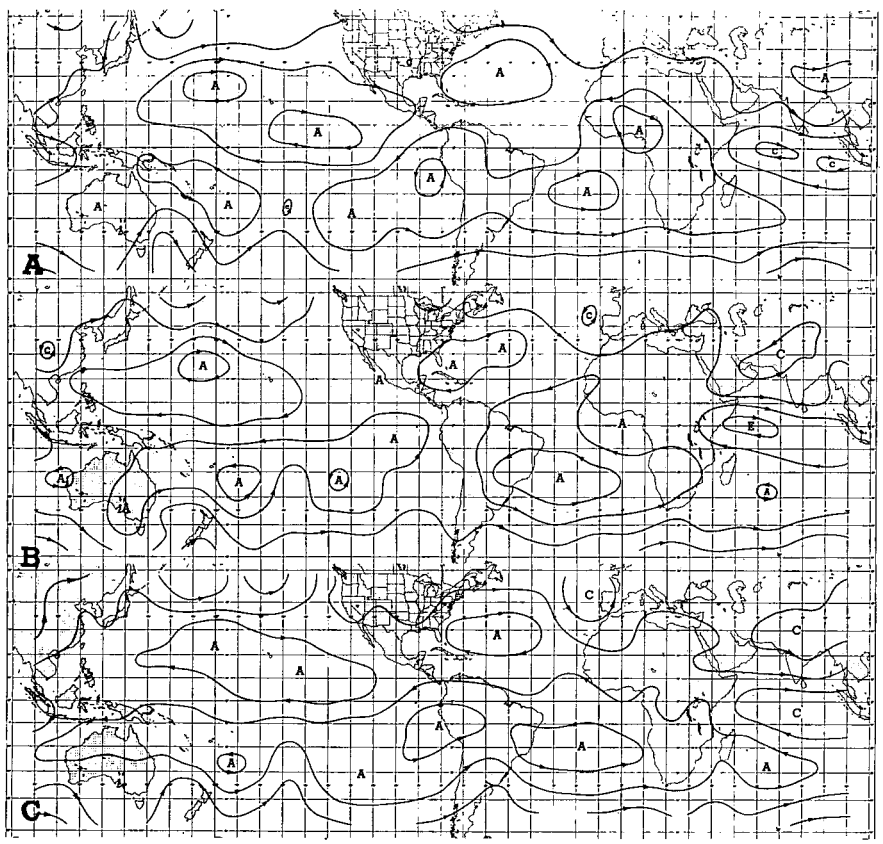

FIGURE 8.—Same as figure 7 for 850 mb.

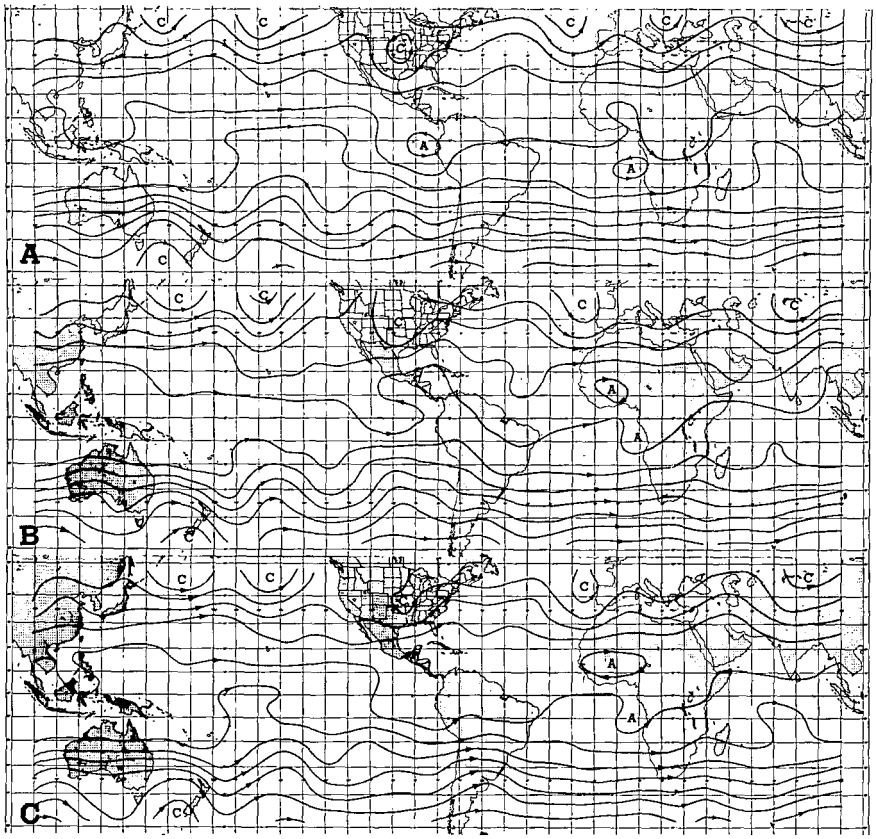

FIGURE 9.—Same as figure 7 for 500 mb.

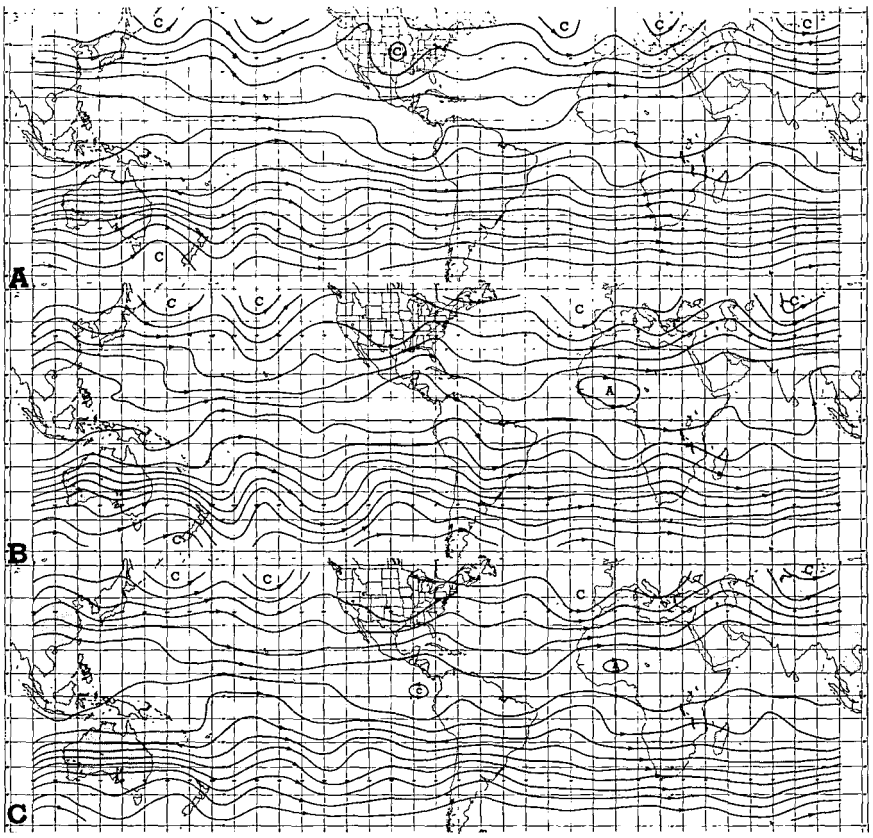

FIGURE 10.—Same as figure 7 for 300 mb.

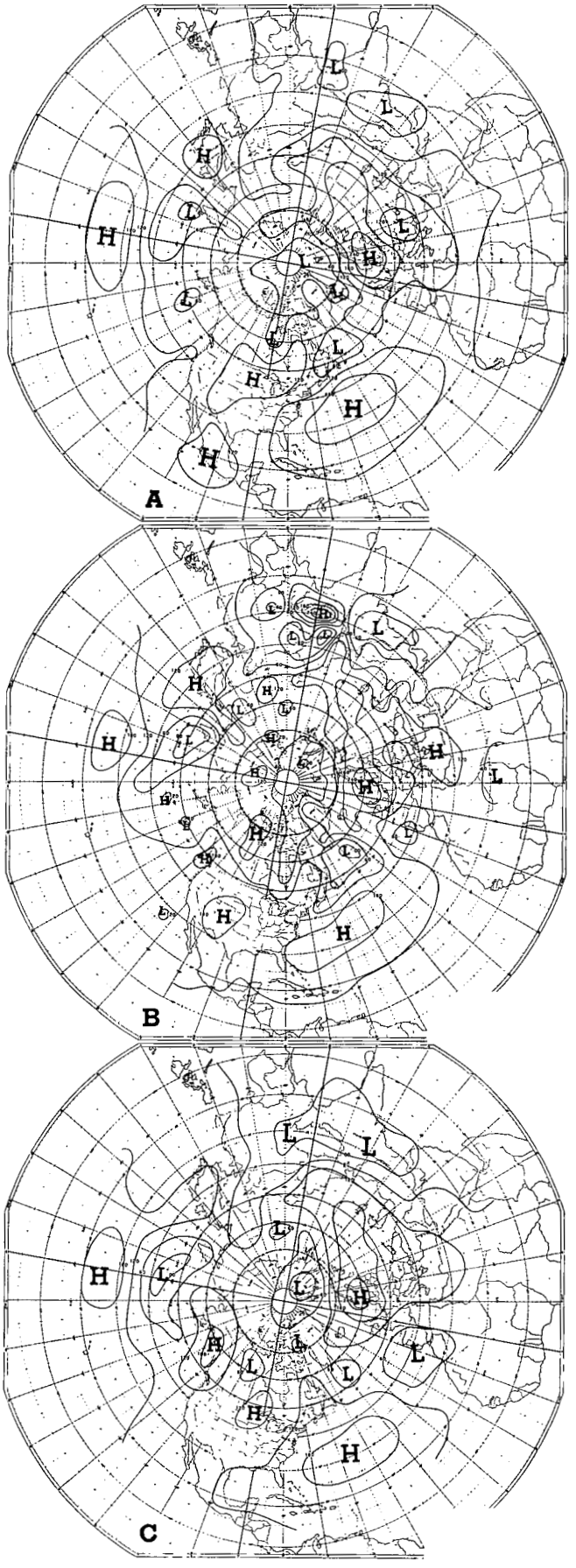

FIGURE 11.—The 1000-mb height field (m) for the Northern Hemisphere: (A) initial, 0000 GMT, June 4, 1970, (B) 24-hr forecast, and (C) verification.

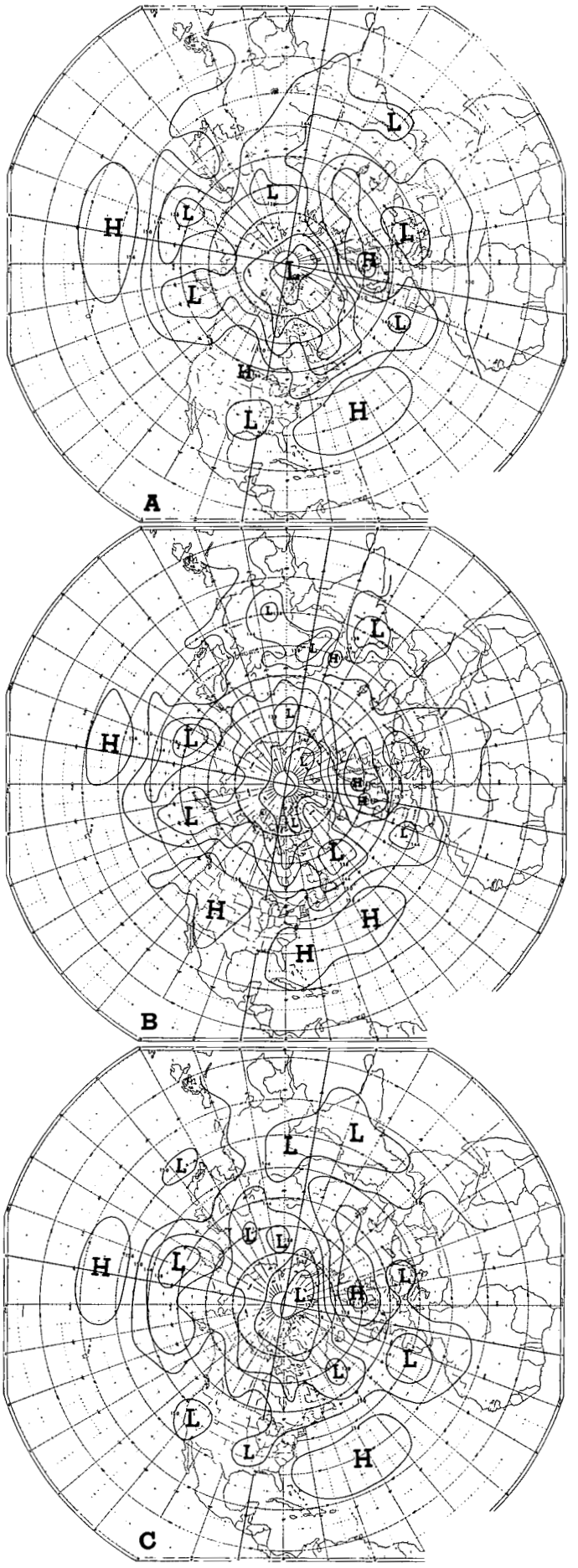

FIGURE 12.—Same as figure 11 for 850 mb.

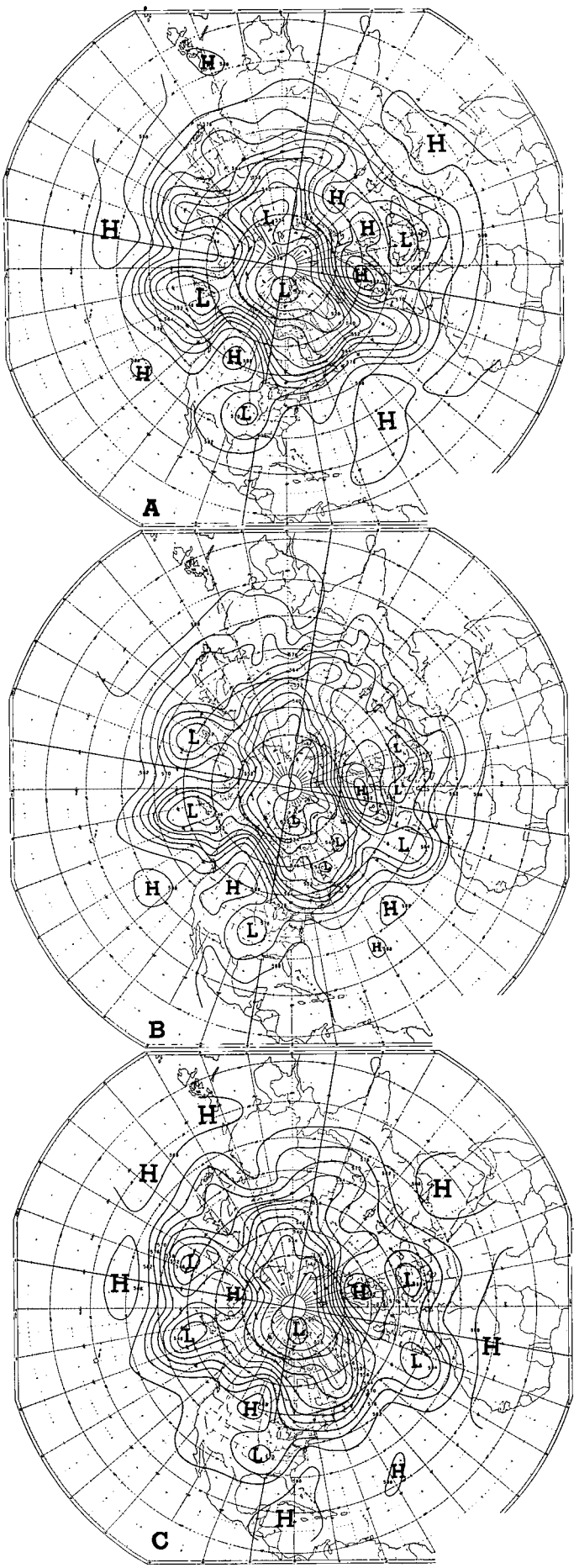

FIGURE 13.—Same as figure 11 for 500 mb.

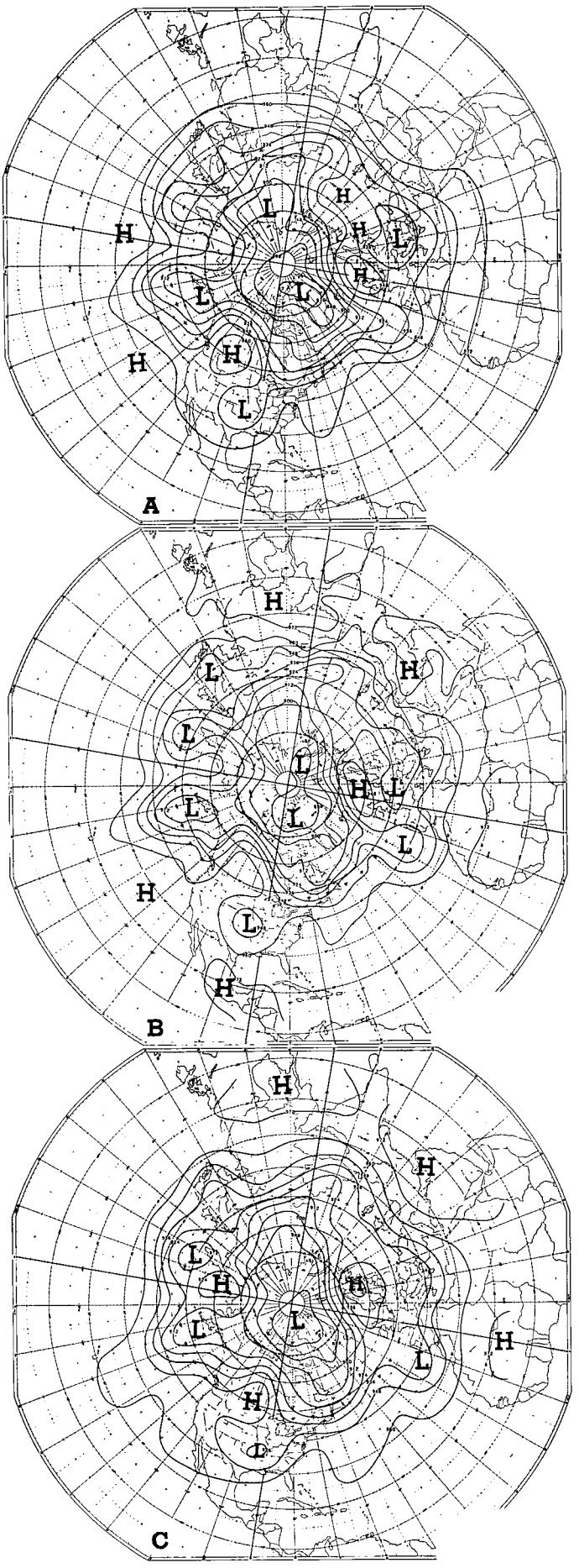

FIGURE 14.—Same as figure 11 for 300 mb.

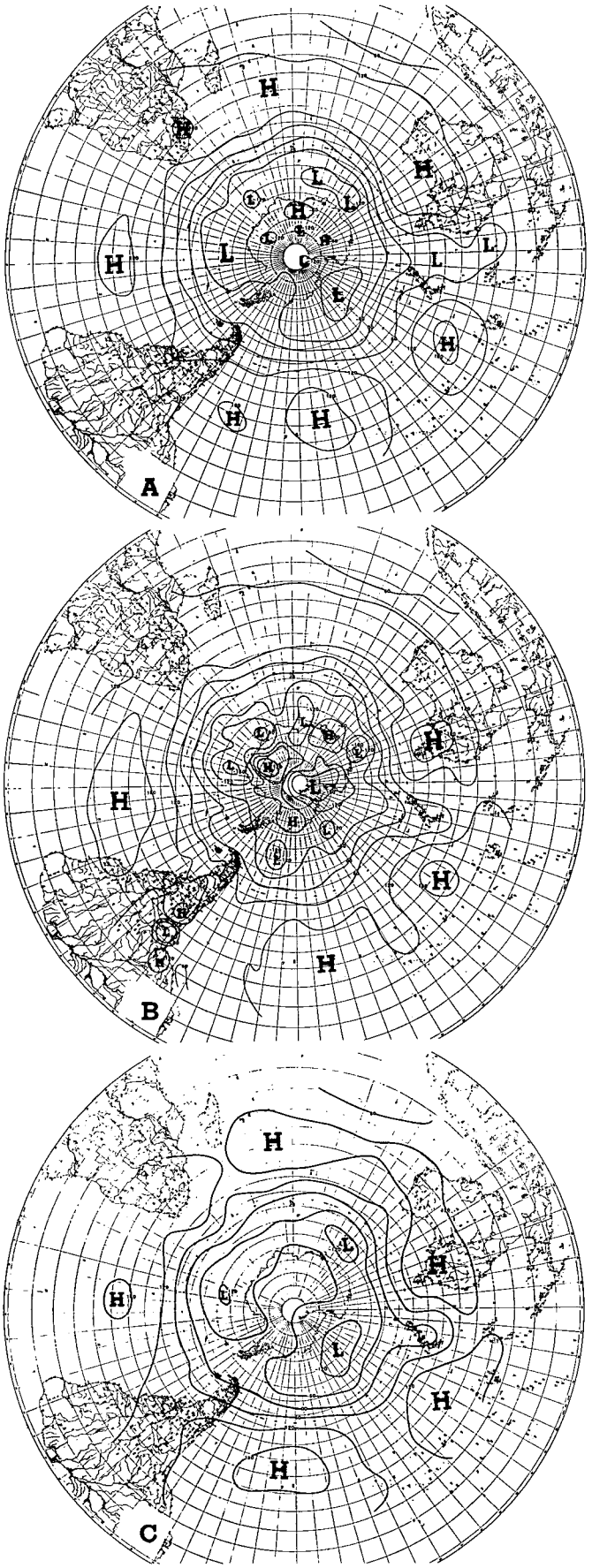

FIGURE 15.—The 1000-mb height field (m) for the Southern Hemisphere: (A) initial, 0000 GMT, June 4, 1970, (B) 24-hr forecast, and (C) verification.

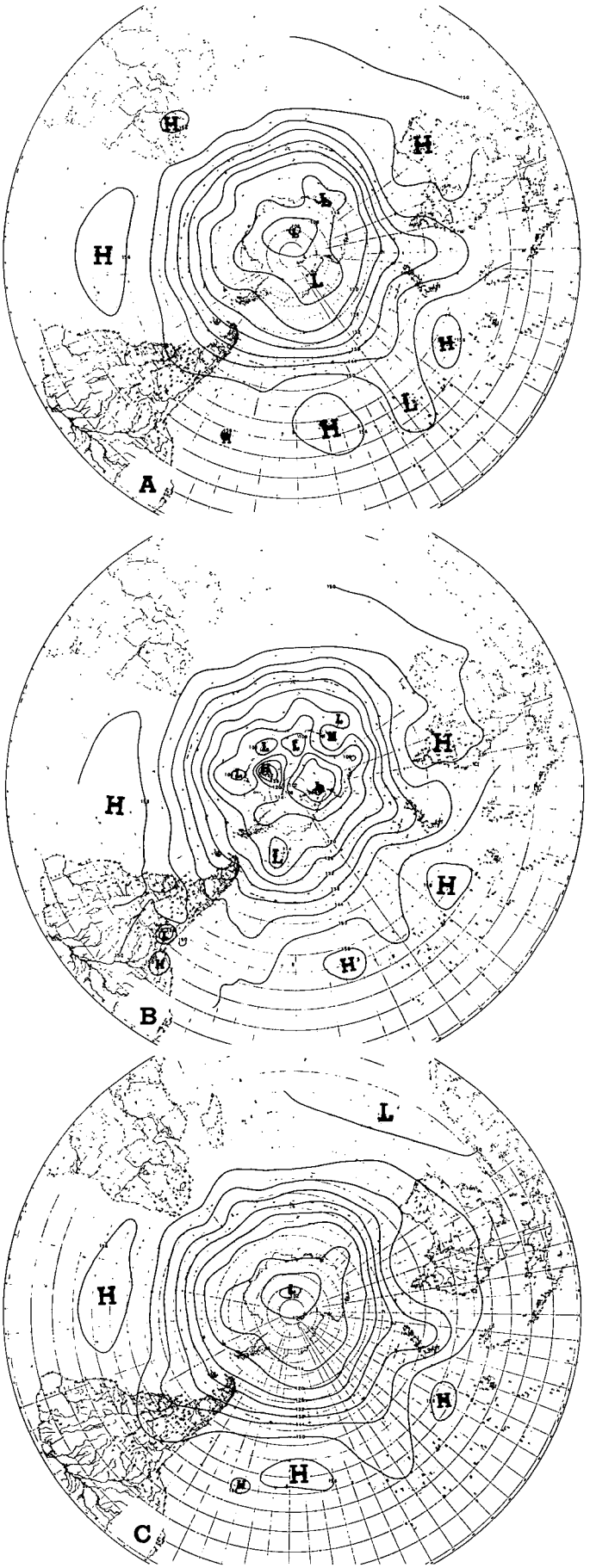

FIGURE 16.—Same as figure 15 for 850 mb.

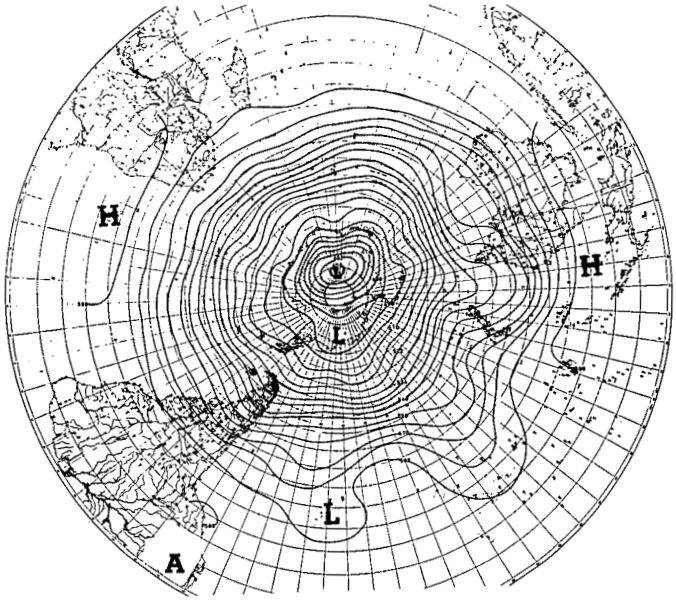

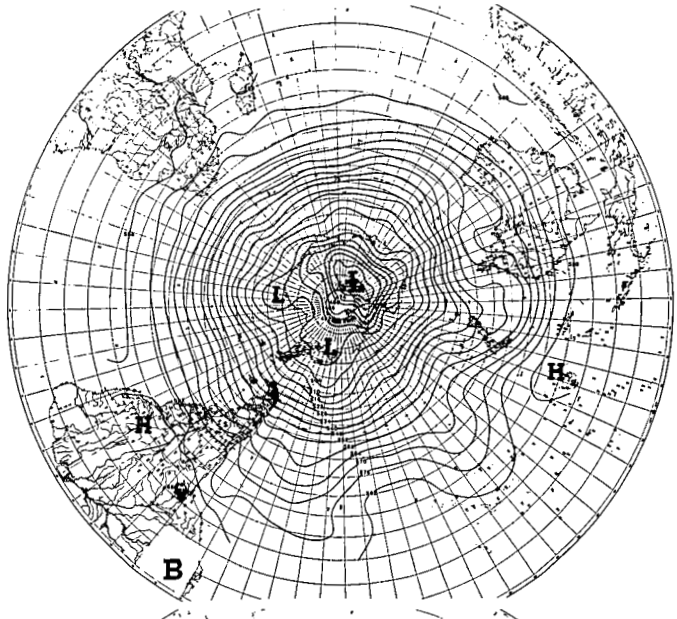

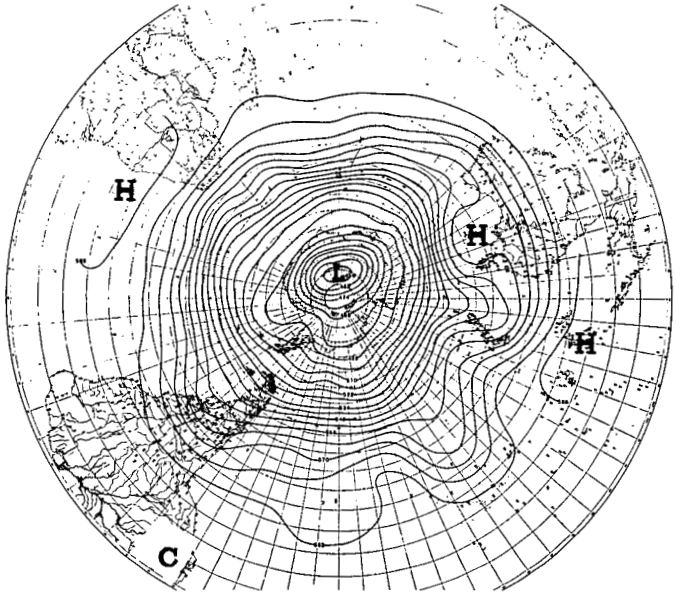

FIGURE 17.—Same as figure 15 for 500 mb.

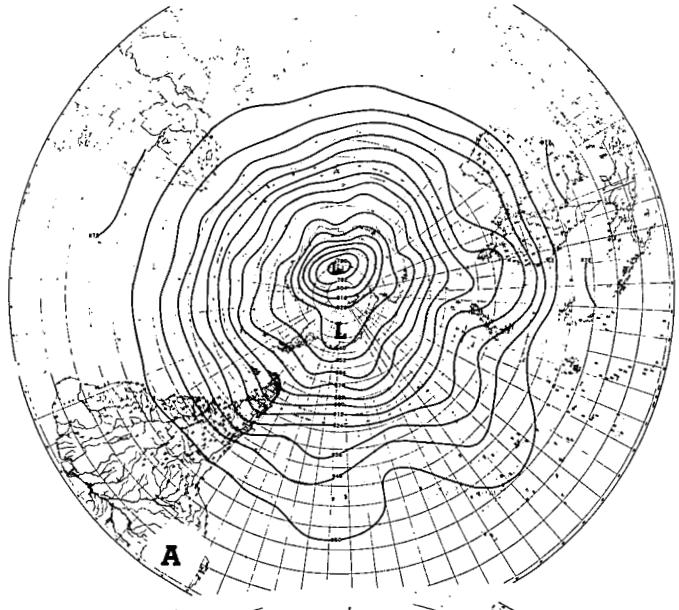

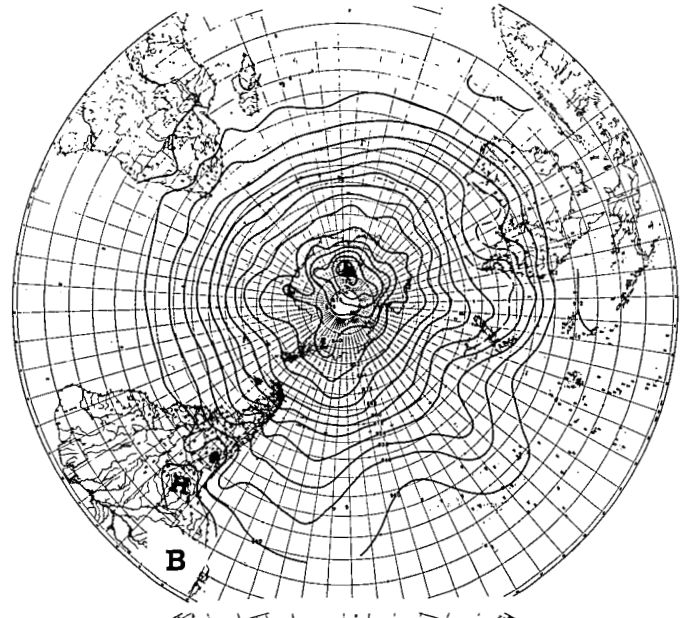

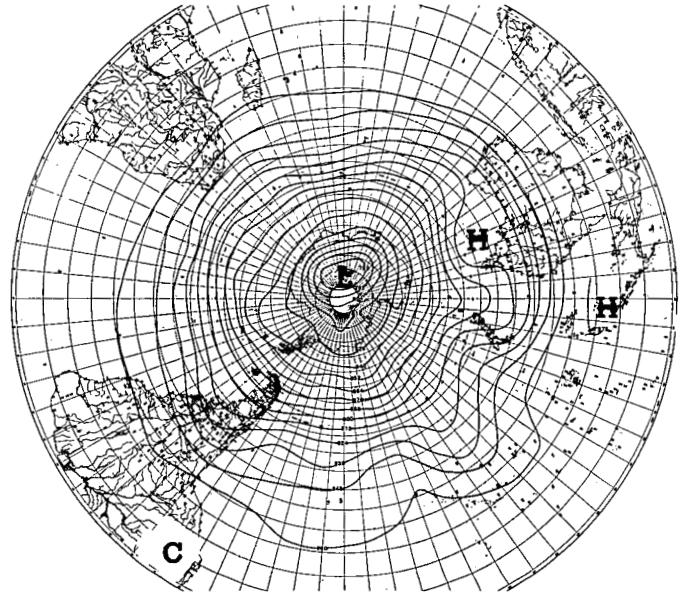

FIGURE 18.—Same as figure 15 for 300 mb.

interpolated from the forecast model to the particular pressures were used.

For the most part, the forecast gives reasonable estimates of the movements of most of the systems. The flow is probably more zonal in the Southern Hemisphere than it should be, due to a zonal first-guess analysis and paucity of data. Problems in the definition of reduction appear in the 1000-mb forecast over the high terrain region of Asia. The effects of terrain in the forecast calculation are most evident and interesting, expecially over the Andes chain at 500 and 300 mb.

6. CONCLUSIONS AND PLANS

An exciting beginning in global analysis and forecasting has been made. The future promises to be even more exciting and interesting. There are numerous problems to be solved and experiments to be made. Accurate analyses will depend on cycling the forecast for a better first guess and good SIRS report coverage, especially in the Southern Hemisphere. Improved means of extracting initial data such that the vertical shear is preserved in the forecast seem necessary. Inclusion of friction, heating and radiation, and moisture and its effects on the forecast will be tested. Energy calculations during progress of the forecast will be included soon.

ACKNOWLEDGMENTS

The author is indebted to F. G. Shuman and J. A. Brown for their encouragement and support during the development of both the global forecast calculation scheme and the three-layer forecast model. The author is also indebted to J. D. Stackpole for his excellent advice and strong recommendation to employ triangular east–west weighting of tendencies and to Robert Y. Hirano for his direct assistance, including programming and testing, in development of the forecast model. S. L. Rosenthal of the National Hurricane Research Laboratory, NOAA, suggested including the stream function figures to better depict low-latitude flow. The author is grateful to T. W. Flattery, who made the forecast possible at this time by supplying his global analysis, and to Mary Daigle, who typed the paper.

REFERENCES

Dey, Clifford H., "A Note on Global Forecasting With the Kurihara Grid," *Monthly Weather Review*, Vol. 97, No. 8, Aug. **1969**, pp. 597–601.

Flattery, Thomas W., "Spectral Models for Global Analysis and Forecasting," *Proceedings of the 6th AWS Technical Exchange Conference, U.S. Naval Academy, Annapolis, Maryland, September 21–24, 1970.* U.S. Air Force, Air Weather Service, Washington, D.C., Apr. **1971**, pp. 42–54.

Nitta, Takashi, and Hovermale, John B., "A Technique of Objective Analysis and Initialization for the Primitive Forecast Equations," *Monthly Weather Review*, Vol. 97, No. 9, Sept. **1969**, pp. 652–658.

Phillips, Norman A., "A Simple Three-Dimensional Model for the Study of Large-Scale Extratropical Flow Patterns," *Journal of Meteorology*, Vol. 8, No. 6, Dec. **1951**, pp. 381–394.

Shuman, Frederick G., "On Certain Truncation Errors Associated with Spherical Coordinates," *Journal of Applied Meteorology*, Vol. 9, No. 4, Aug. **1970**, pp. 564–570.

Shuman, Frederick G., and Hovermale, John B., "An Operational Six-Layer Primitive Equation Model," *Journal of Applied Meteorology*, Vol. 7, No. 4, Aug. **1968**, pp. 525–547.

Staff, NMC (National Meteorological Center), "A Global Numerical Prediction for Apollo 13," *Bulletin of the American Meteorological Society*, Vol. 51, No. 7, July **1970**, pp. 594–601.

Vanderman, Lloyd W., "Operational Programs and Research and Development for Tropical Forecasting at the National Meteorological Center," *Proceedings of the Working Panel on Tropical Dynamic Meteorology, August 7–September 1, 1967, Monterey, California, NWRF* 12–1167–132, Navy Weather Research Facility, Norfolk, Va., Nov. **1967**, pp. 77–96.

Vanderman, Lloyd W., "Global Forecasts on a Latitude-Longitude Grid With Primitive Equation Models," *Proceedings of the International Seminar of Tropical Meteorology, Campinas, S.P., Brazil, September 25–October 10, 1969*, Escritorio de Meteorologia (M.A.), Brasilia, Brazil, **1970**, pp. 233–269.

[Received May 19, 1972; revised August 31, 1972]